Numerical Analysis of Forced Convection for Staggered Cylinders Submerged in Packed Bed Porous Media.

Volume :6 year: 2024

مجلة العلوم والتطـبيقات الهـندسية
Journal of Science and Engineering Application
ISSN 2521-3911

Numerical Analysis of Forced Convection for Staggered Cylinders Submerged in Packed Bed Porous Media.

Enas Khudhair [1, a]
and Dhamyaa.
Khudhur [1, b]
1Department of Power Mechanics Technical
Engineering Technical College of Najaf,
Najaf, Iraq.
[a]E-mail address: enas.abdul.cnj@atu.edu.iq
[b]E-mail address: damiaamech@uomustansiriyah.edu.iq

KEYWORDS
Heat transfer, Porous packed beds, submerged cylinders, staggered patterns.

ABSTRACT
Heat transfer in porous media is a topic that has received great attention in the scientific community in recent decades. In this work, the effect of changing the diameters and porous materials on the heat transfer rate and pressure drop in an iron channel with cross-sectional dimensions (10 × 10) cm and length (240 cm) was studied at Reynolds numbers between (1100 to 2250) with a constant heat flux of 2000 W/m^2, and the cross-sectional dimensions of the test section were (10 × 10) cm, and the length was (30) cm numerically. Three porous materials with different diameters are used, Alumina with diameter (4-6 mm), Silica Gel with diameter (4-2 mm) and Molecular sieve with diameter (3-2 mm). The air flow directed through eight rows of cylinders in staggered arrangement, each with a diameter of 15 mm and a length of 10 cm, immersed in a porous packed bed.
The results showed that Alumina partial has a greater capacity to absorb the heat generated around the cylinders because it has greater thermal conductivity and porosity than Silica Gel and Molecular sieve. According to research, increasing air velocity from 0.187 m/s to 0.35 m/s increases the mass flow rate; resulting in a large heat transfer between the airflow and the cylinders. Also, the increase of the diameter of the porous particles, is decreases in the pressure drop.

Introduction

Many academics are interested in the subject of forced convection heat transport around a body submerged in a porous media due to its significance in numerous engineering and geophysical applications (Nield and Bejan 1999) [1]. the porous media is utilized in various applications, including insulation, heat exchangers, solar energy storage, nuclear power plant, drying and building materials (Bejan, et al. 2004) [2]. Many scholars have mathematically studied optimizing heat transmission from packed cylinders using a porous material. Few numerical studies exist about porous circular cylinders' heat transfer and fluid flow. The earlier studies focused on evaluating the overall heat transfer rate rather than fluid flow.
(Andrew Rees, et al.2004)[3] studied the effect of a stable-temperature cylinder perpendicular to a steady fluid stream in porous material on forced convective heat transfer. The boundary layer thickness was quite low when the Péclet number ’s was very high. The lack of topical thermal equilibrium between the fluid and solid phases impacted the cylinder's heat transfer rate. In every situation, fluid surface heat conduction is higher than the solid matrix.
(Layeghi and Nouri-Borujerdi, 2004) [4] studied fluid flow and heat transmission around a porous cylinder at lower and intermediate Peclet numbers. Darcy's model compares numerical results to literary data to understand heat transfers and fluid flow inside a porous media through a uniform cylinder. Fluid and heat transmission in porous media were investigated using the Darcy model. The numerical method was effective enough for Peclet numbers below 40.
(Gazy F. Al-Sumaily et al. 2010) [5] studied forced convective heat transfers from a single circular cylinder in a packed bed of spherical particles. They compared heated cylinders with and without porous material. Due to thermal dispersion, a porous material increases heat transport at a high Reynolds number. Re affected Nu more than the thermal conductivity of solid/fluid in the porous channel Particles raise cylinder heat. (H.Y. Li, et al. 2010) [6] examined heat transmission and fluid flow inside the channel at staggered porous blocks Navier-Stokes and Brinkmane-Forchheimer equations sample fluid flow in porous sections. Different factors affecting fluid speed were analyzed, including the Reynolds number, Darcy number, height, and width of the porous block. The algorithm of SIMPLER was able to disentangle the relationship between the pressure and velocity fields. As shown by the results, raising the relative thermal conductivity between the porous blocks

and the fluid significantly improve heat transmission at the locations of the porous blocks.

(Khaled Al-Salem, et al. 2011) [7] studied experimentally to determine the thermal impact of wrapping a porous aluminum sheet around a circular tube. The experimental instrument is a heated horizontal cylinder. Different-thickness porous sheets are then wrapped around the cylinder. Varying air velocity crosses the tube, resulting in different Reynolds numbers. The porous layer's influence on cylinder pressure loss was also studied. A porous layer improves heat transfer. The porous layer doesn't increase pressure loss.

(P. Foroughi, et.al, 2011) [8] examined numerically local thermal non-equilibrium (LTNE) conditions, pulsatile and steady flow, and heat transfers inside a channel lined with two porous layers. Heat transfer in porous media improved by raising the solid's relative thermal conductivity to the fluid's thermal conductivity. The Nusselt number, which has a minimum frequency for each amplitude of pulsation, may rise if the amplitude of the pulsation increase.

(Xu et al. 2011) [9] examined the analytical solution of fully formed forced convection in a tube containing open-celled metallic foams. The Brinkman flow model describes fluid transport in the foam region, and the local thermal non-equilibrium model represents fluid-solid energy exchange. Interfacial temperature coupling conditions are proposed and used to generate an analytical solution. This solution gives temperature profiles and velocity with exact friction and Nusselt numbers.

(Nimvari, et al. 2012) [10] studied heat transport and turbulent flow numerically in a porous channel, and porous layer layouts were central and boundary. It analyzes porous layer thickness and Darcy number. Turbulent kinetic energy peaks at porous/fluid interface. Due to channeling, the thickness is different in the middle and edges. The balancing Nusselt number and pressure drop determine the ideal porous layer thickness.

(Gazy. Al-Sumaily and Thompson, 2012) [11] studied time impacts on forced convection heat transfers about a cylinder submerged in spherical particles. Thermal dispersion and non-Darcian effects were considered. Heat transfer rates, thermal responses, and hydrodynamics were evaluated for various Reynolds numbers as a function of the porous material's presence and thermal properties: relative thermal conductivity from solid-to-fluid (0.01 to 1000) and Biot number (0.01 to 100). (1 to 250). The result showed that porous particles minimized wakes beyond the cylinder and enhanced heat transmission.

(Thompson and Gazy. Al-Sumaily., 2013) [12] Simulated constant and pulsatile forced convective fluxes in a porous horizontal channel. The porous-material-filled channel used Darcy–Brinkmann–Forchheimer momentum and two-equation energy models; the empty channel used Navier–Stokes equations. This study uses Reynolds numbers (1–250) and porous materials with thermal conductivity (kr = 0.1, 1.0, 10, 100). Stable and unstable wakes occur in an empty channel as the Reynolds number rises. Reynolds number, oscillation amplitude, and forcing frequency affect time-dependent periodic and quasi-periodic shedding. Simulations of porous-medium-filled channels increased flow. The cylinder did not produce any wakes.

(Gazy. Al-Sumaily,2014) [13] studied how transverse spacing, the porous medium's thermal conductivity, and Reynolds number influence flow and heat transmission about four heated cylinders in in-line and staggered arrangements. For three solid/fluid thermal conductivity rates (1.725 - 57.5- 248) and variable Reynolds numbers (1- 250), the influence of cylinder center distance (SP = 1.5 and 3.0) on local and average heat transfer was examined in all configurations. Reynolds numbers, SP, and cylinder layout affect average and local Nusselt numbers. Thermal conductivity ratios in both cylinder forms do not alter average Nusselt number changes with SP. The staggered arrangement gives greater thermal performance than in-line.

In an experimental and computational (Sandeep Koundinya, et al. 2016) [14] studied fluid and heat flow characteristics in porous media. Porous media included a tube containing a hollow inner in which packed alumina balls were put in a specific way. The result of CFD showed that the pressure drop was proportional to inflow velocity in both simulations and experiments and inversely commensurate to particle diameter and porosity.

(Habib Sayehvand,et al,2017) [15] studied the effect of changing the horizontal space between two sequential circular cylinders embedded in spherical aluminum particles on the flow pattern and heat transfers. The fluid out temperature and the total wall heat fluxes from two circular cylinders embedded in a packed bed raised to a maximum before decreasing with a negative gradient. Porous media considerably raises the pressure drop but enhances their ability to absorb heat from two cylinders. The result showed that the wall heat flux was low when the space between the two sequential cylinders was short, as in the case of an empty channel.

(Brijendra and Choudhary, 2017) [16] examined the thermal performance of a metal foam heat exchanger, including heat transmission and pressure drop. Experimental data was visually shown, such as friction factor, efficiency, Reynolds number, and Nusselt number. Reynolds number 900 maximizes heat transfer. According to a study, the most efficient heat exchanger at (ε=30%, u = 0.2 m/s) also had the lowest operating temperature.

(Mahboobe, et al.,2018) [17] examined theoretically hydrodynamics and heat transport through a porous woven copper wire-made pipe with a uniformly heated pipe wall. Analyzed how changes in porous medium thickness, Reynold number, and thermal conductivity ratio affected heat transmission. In contrast to cases

where a porous insert was not used, there is no pressure drop and better heat transfer at higher Reynold numbers in the laminar regime.

(Sharma, et al., 2020) [18] used analytical and numerical methodologies to explore the flow and heat transmission inside a straight tube filled with porous media. To depict constant incompressible viscous fluid flow through a porous material, Darcy and the Brinkman equation [19] are utilized, and the results are compared. A homogeneous/heterogeneous porous material, as well as a uniform heat flow boundary condition, was taken into account. The Darcy model has been proven to give an upper constraint on Nusselt number in both homogeneous and heterogeneous porous media. COMSOL Multiphysics numerical simulations are used to verify the theoretical results.

(Chanmak1.et al.,2021) [20] measured the experimental friction factor (f) and Nusselt number (Nu) in a circular tube under uniform heat fluxes. Stainless steel wire mesh was the porous medium. Reynold number ranges (3000-15000), and Plates were 10–50 mm apart (p). The result shows Nu rising as Re and the space between two wire mesh (p) plates drops, resulting in increased material mass and heat transmission to the pipe wall by storing more hot air energy.

This study investigates the fluid and heat transport over a submerged cylindrical porous media in a horizontally two-packed bed (alumina, silica gel, and molecular sieve). Three-dimensional numerical simulations show a forced convective flow of a viscous, incompressible, and laminar fluid across a staggered configuration of eight cylinders submerged in a horizontal porous packed bed. The cylinders are heated at a constant rate (2000 W/m^2), and the working fluid is air moving at three different speeds (0.187, 0.24, and 0.35 m/s).

Numerical Investigation

2.1 The physical model

The current research looked at the airflow and heat transfers from cylindrical tubes submerged in a horizontal porous media-packed bed filled with spherical particles (alumina, silica gel, and molecular sieve). As illustrated in Fig. (1), the physical mode consists of a channel having an inlet portion, an entry section, a test section, and an output section. The air duct has a square cross-section with a length of (240) cm and a square cross section (10×10) cm. The cross sectional dimensions of the test portion are (10 ×10) cm, and the length is (30) cm. The porous channel's geometrical structure is shown in Fig. (2) and consists of two porous packed beds; each packed has a cross section of (10 x 10) cm and a length of (5) cm. Three gaps are used between the two permeable porous beds with a distance of (5) cm. The distances between the first and third gaps are (75) cm of the test section. Also, in the test part, air flows over eight cylindrical tubes of 15mm diameter and 10 cm length submerged in a horizontal porous packed bed, as shown in Fi (3) .The cylinders are heated at a steady rate (2000 W/m^2). The working fluid is air at three velocities (0.187, 0.24, and 0.35) m/s. Table 1 illustrates the permeability, thermal conductivity, diameter, and porosity of the porous media used in this investigation.

Table 1: Porous media porosity and thermal characteristics

Material	Diameter (mm)	Permeability (m^2)	Thermal conductivity (W/m. k)	Porosity ε
Alumina	6	4.5918x10^{-8}	20.96323	0.41798
	4	1.8984x10^{-8}	21.6065	0.4001
Silica gel	4	1.8984x10^{-8}	0.84992	0.4001
	2	3.9007x10^{-9}	0.87453	0.3822
Molecular Sieve 13X	3	2.47576x10^{-8}	0.16425	0.39112
	2	3.9007x10^{-9}	0.166283	0.3822

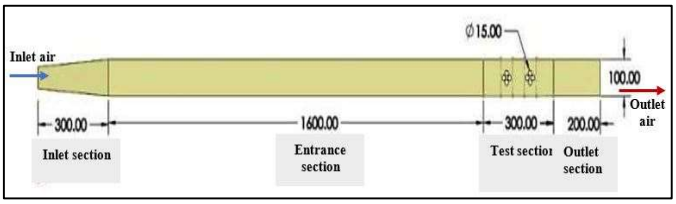

Fig. 1: The geometrical of the present model

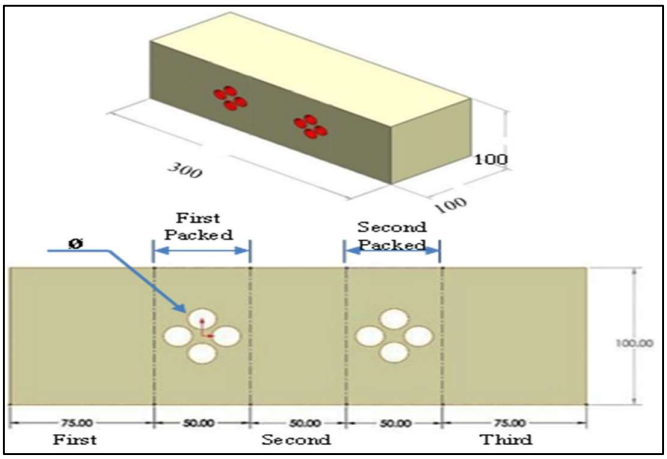

Fig. 2: Test section of present model

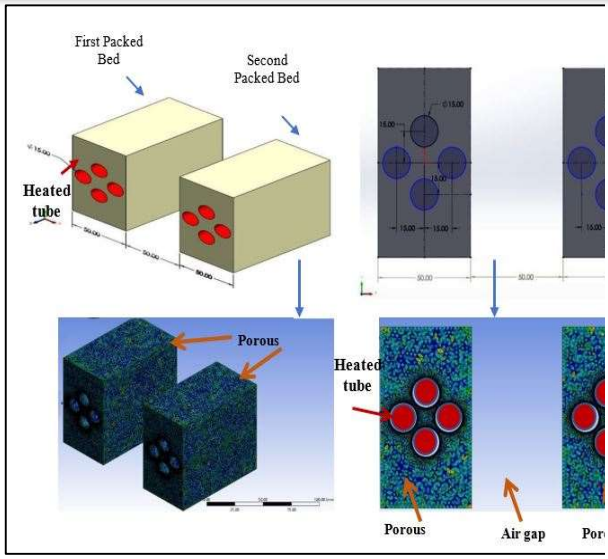

Fig.3: Packed porous bed with heated tubes

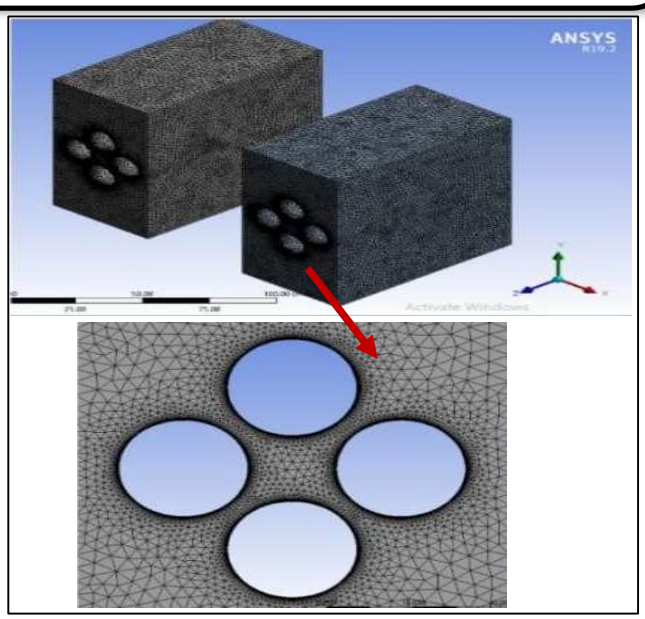

Fig.5: The mesh of porous packed bed

2.2 The Mesh generation

In order to maintain grid independence, the porous channel and two porous packed beds each had a characteristic mesh size. Fig (4) shows the computational grid in the (x, y, and z) orientation used to design the geometric parameters of a porous channel.

The meshes of the suggested geometry for two porous blocks with cylindrical tubes immersed in a horizontal porous packed bed in staggered patterns examined in this paper are displayed in Fig (5).In the present case, an average of (3120337) elements and (741109) nodes are used after several attempts. This study used 1000 iterations, but the convergence happened at iteration 300.

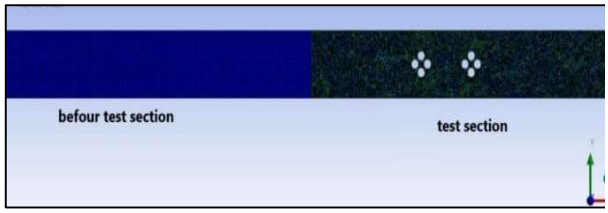

Fig.4: Mesh generation of test section

2.3 The governing equations

Before starting to analyze cases, it is a good idea to state the governing equations' assumptions:

- Steady-state
- Incompressible fluid
- Newtonian flow.
- Laminar flow The Reynolds number rang, 1100 ≤ Re ≤ 2250
- Three dimensions
- Constant heat flux

This work determines the temperature profiles using computational fluid analysis (CFD). The computational fluid dynamic (CFD) is used to give the best model that can be made experimentally without the need for costly prototypes.

The conservation of mass, momentum, and energy equations, as well as the governing differential equations of fluid flow and heat transmission, have been illustrated. All of the equations are displayed in a Cartesian coordinate system.

2.3.1 Conservation of mass:

This research used the 3-D Navier-Stokes governing equations for an incompressible fluid. For the fluid domain, the mass continuity equation is [20].

$$\frac{\partial u}{\partial x}+\frac{\partial v}{\partial y}+\frac{\partial w}{\partial z}=0 \qquad (1)$$

2.3.2 Momentum Conservation

The other basic set of equations that control fluid flow is derived from Newton's second law (the conservation of momentum). Darcy-equilibrium equations or full instantaneous equations for an incompressible fluid are the names of the equations [21]:

The x- momentum equations

$$\frac{1}{\varepsilon^2}\left[u\frac{\partial u}{\partial x}+v\frac{\partial v}{\partial y}+w\frac{\partial w}{\partial z}\right]-\frac{1}{\rho f}\frac{\partial p}{\partial x}+\frac{1}{\varepsilon^2}\,veff\left(\frac{\partial^2 u}{\partial x^2}+\frac{\partial^2 u}{\partial y^2}+\frac{\partial^2 u}{\partial z^2}\right)-\frac{vf}{k}+\frac{\varepsilon C}{\sqrt{k}}\left|\vec{V}\right| \quad (2)$$

The y- momentum equations:

$$\frac{1}{\varepsilon^2}\left[u\frac{\partial u}{\partial x}+v\frac{\partial v}{\partial y}+w\frac{\partial w}{\partial z}\right]=-\frac{1}{\rho f}\frac{\partial p}{\partial y}+\frac{1}{\varepsilon^2}veff\left(\frac{\partial^2 v}{\partial x^2}+\frac{\partial^2 v}{\partial y^2}+\frac{\partial^2 v}{\partial z^2}\right)-\left[\frac{vf}{k}+\frac{\varepsilon C}{\sqrt{k}}\left|\vec{V}\right|\right]v \quad (3)$$

The z- momentum equations:

$$\frac{1}{\varepsilon^2}\left[u\frac{\partial u}{\partial x}+v\frac{\partial v}{\partial y}+w\frac{\partial w}{\partial z}\right]=\frac{1}{\rho f}\frac{\partial p}{\partial z}+\frac{1}{\varepsilon^2}veff\left(\frac{\partial^2 w}{\partial x^2}+\frac{\partial^2 w}{\partial y^2}+\frac{\partial^2 w}{\partial z^2}\right)-\left[\frac{vf}{k}+\frac{\varepsilon C}{\sqrt{k}}\left|\vec{V}\right|\right] \quad (4)$$

Where:

$\left|\vec{V}\right|$: Dimensionless absolute velocity.

$veff$: Effective kinematic Viscosity.

C : Constant.

2.3.3 Energy Conservation

In a non-dimensional formation, the governing equation for energy is defined as [21]:

$$u\frac{\partial T}{\partial x}+v\frac{\partial T}{\partial y}+w\frac{\partial T}{\partial z}=\frac{k_{eff}}{(\rho C_P)f}\left(\frac{\partial^2 T}{\partial x^2}\right)+\left(\frac{\partial^2 T}{\partial y^2}\right)+\left(\frac{\partial^2 T}{\partial z^2}\right) \quad (5)$$

u, v, and w are the velocities in the x, y, and z directions. T the temperature and fluid density.

2.4 Boundary conditions

Boundary conditions are set at the intake; when the fluid enters the duct at a fixed velocity and temperature, assuming the flow is fully formed, the pressure outlet can be located at the outlet.The exterior surface of the domain is an effective thermal insulator, keeping the air inside at a comfortable 298K. A steady heat flux (q = 2000 W/m^2) is applied to the cylinder walls submerged in the porous material. The entrance air velocity to the test channel is in the range of (0.187 to 0.35) m/s, and boundary conditions are considered in this analysis**.**

Boundary conditions are present at the inlet:

$T= T_{in}$=298K, u = v =0

Boundary conditions are present at the outlet:

$P=P_{out}$, u = v = 0, $\frac{\partial T}{\partial z}=0$

Boundary conditions at the walls are:

u = v = w = 0, $\frac{\partial T}{\partial x}=\frac{\partial T}{\partial y}=0$

Boundary conditions at the heat flux surface are:

u = v = w = 0, $q=-k_s\frac{\partial T}{\partial y}$

When porous media was present, a porous zone was chosen, with porosity values of ε (0.382, 0.391 and 0.400) for Silica gel, Molecular Sieve 13X, and Alumina, respectively. This study's offered geometry and flow direction are shown in Fig (6) . The solution becomes convergent when the residuals are less than 10^{-6}, as illustrated in Fig (7).

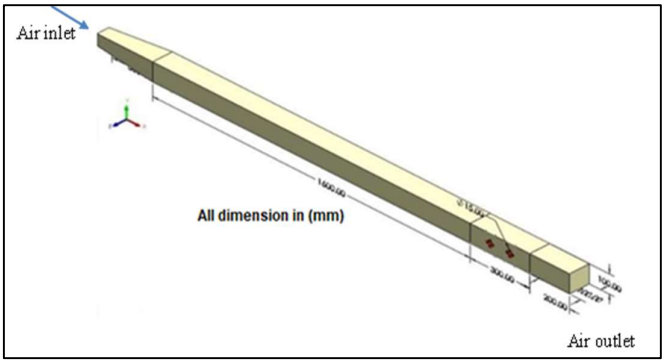

Fig.6: Suggested flow direction and shape

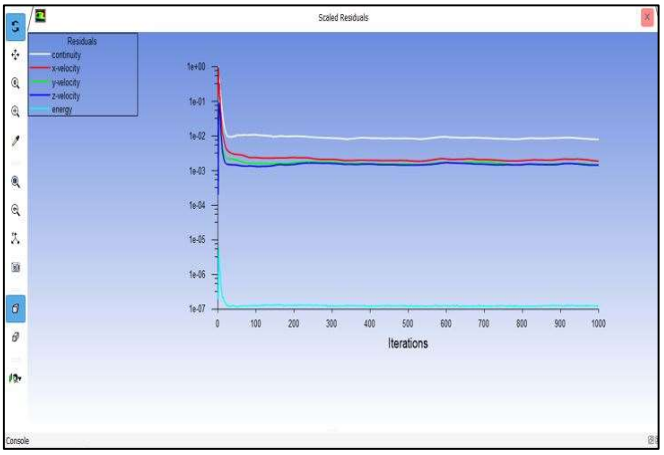

Fig.7: the solution residuals

Numerical Results and Discussion:

Three types of porous media (Alumina, Silica Gel, and Molecular Sieve 13X) were investigated using numerical ANSYS FLUENT version 19.2 software. The channel's temperature contours, velocity vector, and pressure contours and two porous baked beds for several porous media types (alumina, silica gel, and molecular sieve 13X) are obtained at Reynold numbers in the range of 1100 to 2250 and heat flux 2000 W/m^2.

The main purpose of this study is to determine porous materials' effects on the convective heat transfer in the fluid and solid phases as well as their thermal fields for flow across four cylinders immersed in a horizontal porous packed bed in a staggered arrangement.

Fig (8) show fluid and solid temperature distribution around a staggered cylinder submerged in Alumina material particles packed bed at 0.187, 0.24, and 0.35 m/s air velocity and 2000W/m^2 heat flux. The thermal conductivity of 6mm Alumina is 20.963 W/m.k. the heat

transfer mechanism in the packed bed is conduction from the cylinder wall to the particles and convective heat transfer from the packing particles to the air.

High-conductivity Alumina plots promote conduction from the cylinder wall to the particles, raise particle temperature, and boost convective heat transfer to the air. Any increase in inlet velocity increases turbulence and decreases thermal boundary layer thickness, causing a high heat transfer rate at constant particle diameter, packing conductivity, and heat flux.

As inlet velocity increases, the fluid temperature increases along the flow direction, and its isotherm lines move closer to the surface of the cylinders, resulting in greater temperature gradients. Thus, steep fluid temperature gradients can be seen on the cylinder surface at high velocity (0.35 m/s) compared with those at low velocity (0.187 m/s).

Fig.(9) illustrates the temperature distribution for Alumina material particles with two diameters of packing (4 mm and 6mm) at 0.187 m/s inlet velocity and 2000 W/m2 heat flux. It can be seen that the temperature distribution decreases by increasing the particle diameter (4mm to 6mm) because of increases in the porosity (0.400 and 0.417), which lends to the heat transfer rate decreasing from the cylinder. It is important to of note that the permeability usually depends on porosity. Any change in porosity changes the temperature distribution around the cylinder, especially near the cylinder wall within the thermal boundary layer, as shown in Fig (9). Therefore, the increase of porosity can increase the permeability, of the heat transfer rate from the cylinder surface decreases.

Fig's (10 and 11) demonstrate fluid temperature distribution for staggered cylinder arrangements with different fluid velocity values (0.24 and 0.35) m/s for Alumina (4mm and 6mm) diameters. These contours illustrate that increasing the velocity from 0.24 m/s to 0.35 m/s increases the mass flow rate, resulting in considerable heat transfer between the air and the heater. When porous media is used to improve the convective heat transfer of the heater element in cross airflow, the heat transfer coefficient of the heating element inside the porous medium is larger than that of the heating element in an empty duct at the same velocity (mass flow).

Fig (12) shows the temperature distribution at velocity 0.35 m/s with different porosity ε (0.382, 0.391 and 0.400) for Silica Gel, Molecular Sieve 13X, and Alumina, respectively. The changes in the diameter of the porous material pores in the range of 0.382 to 0.400 showed that increasing the diameter of the pores increases the permeability and the turbulent flow vortices in the porous medium, thereby increasing the turbulence of the flow and reducing pressure drop. For this reason, the smaller the porous media porosity will make it more difficult for air to enter into porous media so that convection heat transfer in the porous media gets, or heat transfer that occurs only takes place by low conduction.

Fig. (13) shows airflow over beds packed with 4mm and 6mm Alumina spheres at 0.187 m/s. As indicated in the figure, the packed bed in the test portion has the highest pressure because it resists airflow. The pressure drop decreases with particle diameter increases (4mm to 6mm).

As expected, solid particles generate a large pressure reduction in fluid flow by interacting with porous particle. With increasing particle diameter, the pressure contours surrounding an eight-cylinder become uniform, especially between eight cylinders, due to no wake between and behind the cylinders.

Fig (14) is shown the pressure drop of airflow through beds packed with spheres of Alumina particles with a diameter (4mm and 6mm) at a velocity of 0.35 m/s. Increasing fluid velocity in a porous channel increases frictional forces from due to resistance. In the porous channel, velocity increases to 0.35 m/s, and the pressure drops approximately six times compared an in Fig.(13) at a velocity of 0.187 m/s. However, the enhanced heat transfer obtained from the porous material is at the expense of a significantly increased unfavorable pressure drop in the packed bed. Also, Fig .(14) is indicated that the increase in the diameter (from 4mm to 6mm) of the porous material leads to an increase of 2.5 times in the pressure drop.

Fig.(15) is shown the pressure contours of airflow through beds packed with different sphere particles of Molecular Sieve 13X, Silica Gel, and Alumina with porosity (ε= 0.382, ε= 0.391 and ε= 0.400) at a velocity of 0.35 m/s. As shown in this figure, pressure drop increases with the decrease of porosity due to the increased air resistance inside the channel.

Fig. (16) is shown the velocity vector of the Alumina with 4mm diameter at velocity (0.187m/s, 0.24 m/s, and 0.35 m/s). This figure is shown that any rising in the inlet velocity tended to raise the turbulence and reduce the thickness of the thermal boundary layer, which caused a high heat transfer rate.

Fig.(17) shows the Alumina's velocity vector with a 6mm diameter at velocity (0.187 m/s, 0.24 m/s, and 0.35 m/s). This figure shows that increasing inlet velocity from (0.187 to 0.35 m/s) forces the fluid to flow from the packed bed region to the outer regions, which reduces the thickness of the boundary layer around cylinders and then increases the heat transfer rate.

Fig. (18) displays the surface temperature distribution of the cylinder for Molecular sieve, Silica, and Alumina at a velocity of 0.187-0.35 m/s. The figure shows that the distribution of the cylinder's surface temperatures for the three materials diminishes as velocity rises with a constant heat source. Additionally, it is noted that the Alumina had a lower temperature on the cylinder surface than Silica Ggel and of Molecular Sieve 13X, respectively. That is because the Alumina has a higher porosity and thermal conductivity than Silica Gel and of Molecular Sieve 13X, which low prevents air from moving through it.

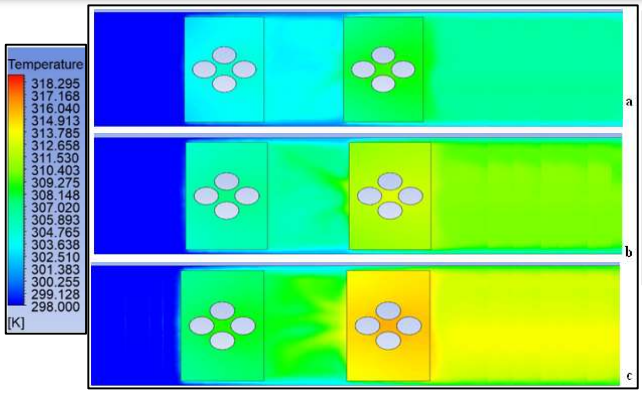

Fig. 8: the Alumina with 6mm diameter temperature contour: a- v= 0.187, b- 0.24, c- 0.35.

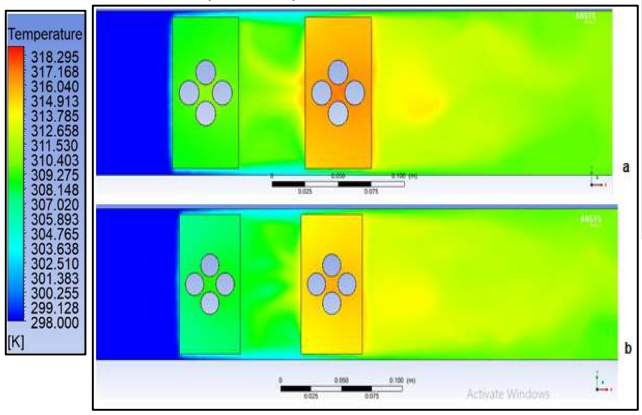

Fig. 9: the Alumina at velocity 0.187 m/s temperature contour with a- 4mm and b-6mm diameter.

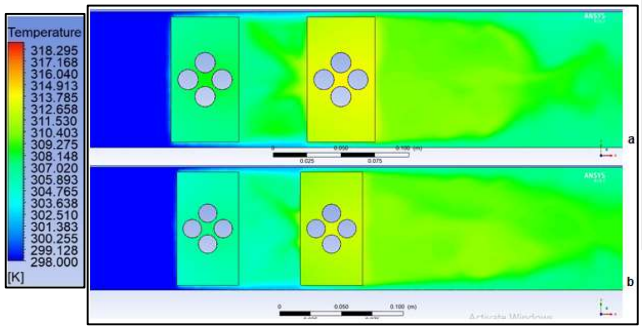

Fig. 10: the Alumina at velocity 0.24 m/s temperature contour with a- 4mm and b-6mm diameter.

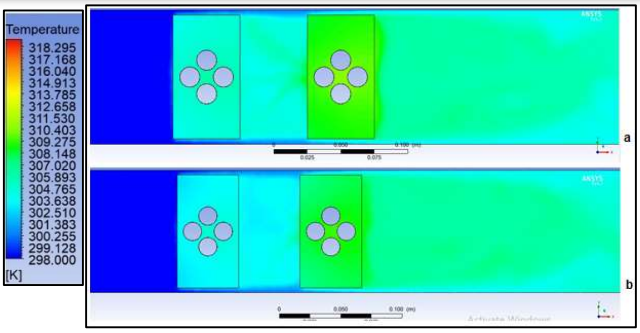

Fig. 11: the Alumina at velocity 0.35 m/s temperature contour with a- 4mm and b-6mm diameter.

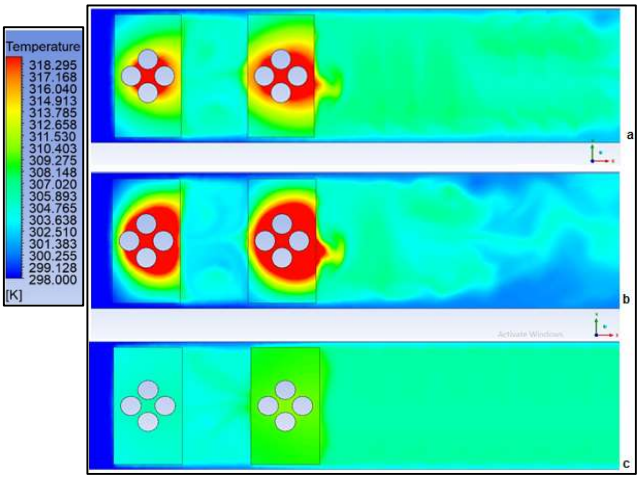

Fig. 12: Temperature contour at velocity 0.35 m/s with a- ε= 0.382, b- ε= 0.391 and c- ε= 0.400.

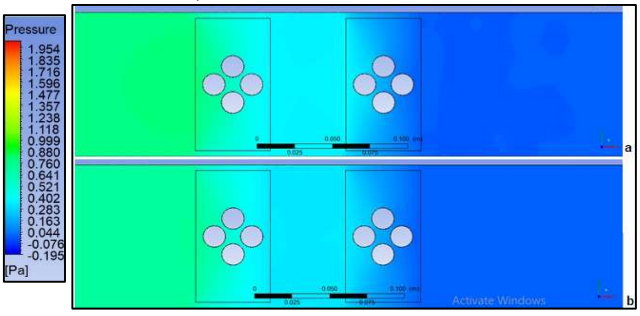

Fig. 13: pressure drop of the Alumina at velocity 0.187 m/s: a- 4mm diameter, b- 6mm diameter

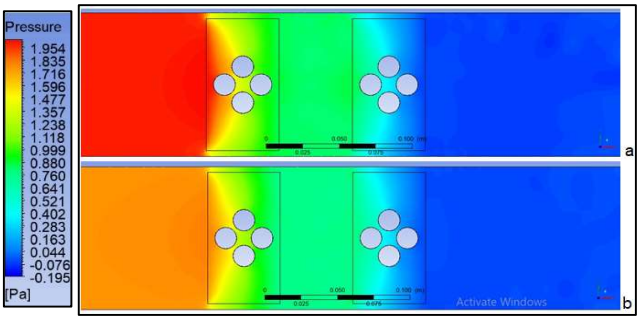

Fig.14: pressure drop of the Alumina at velocity 0.35 m/s: a- 4mm diameter, b- 6mm diameter

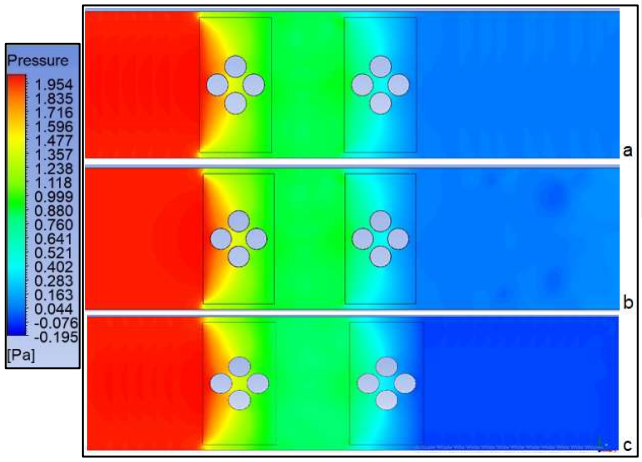

Fig. 15: Pressure contour at velocity 0.35 m/s with a- ε= 0.382, b- ε= 0.391 and c- ε= 0.400.

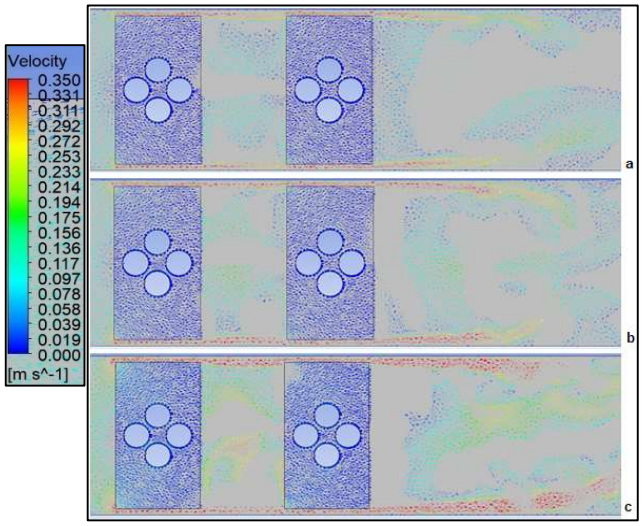

Fig. 16: Velocity vector of the Alumina with 4mm diameter: a- v= 0.187m/s, b- 0.24 m/s, and c- 0.35 m/s.

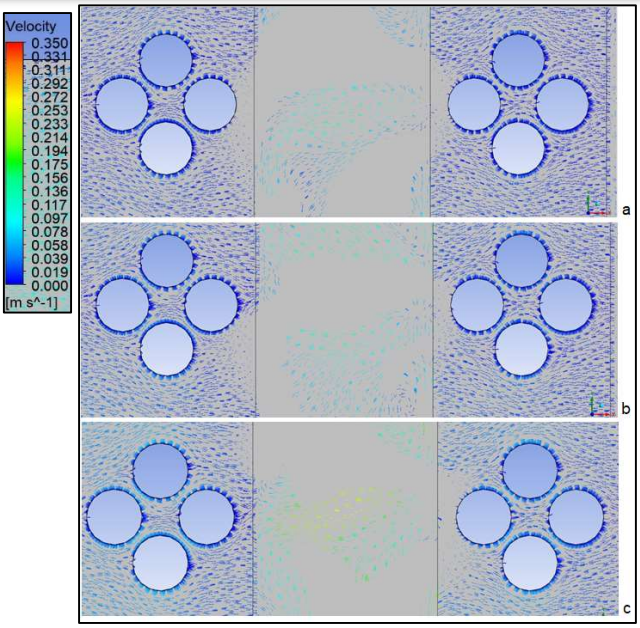

Fig. 17: Velocity vector of the Alumina with 6mm diameter: a- v= 0.187m/s, b- 0.24 m/s, and c- 0.35 m/s.

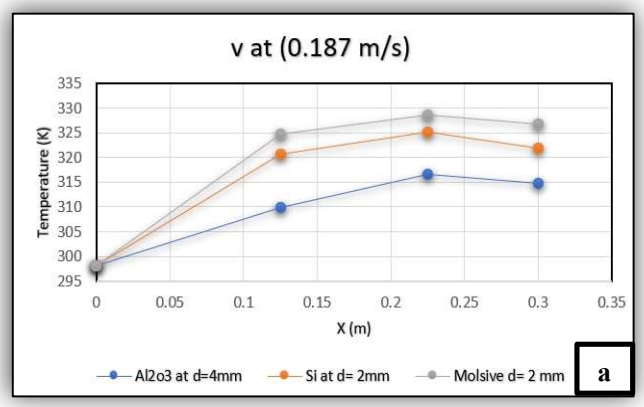

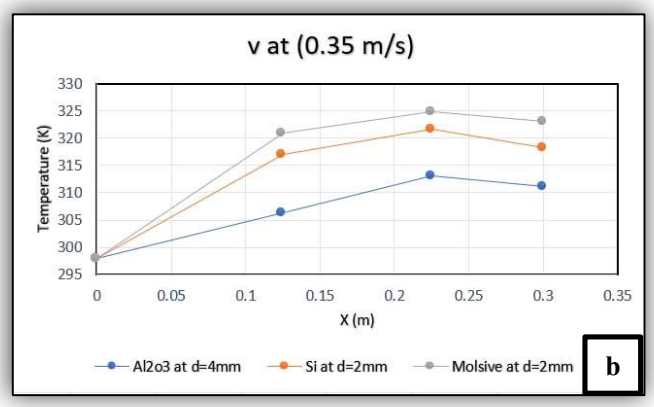

Fig.18: the surface temperature distribution for molecular sieve, silica gel and alumina at a- v= 0.187 m/s, b- v= 0.35

A	Surface area of test section,	mm^2
A_c	cross section of duct,	mm^2
D	Diameter,	mm
ε	Porosity	---
k	Thermal conductivity,	W/m. K
p	pressure drop,	Pa
T	Temperature,	°C
u	velocity of air,	m/s
$\dot{Q}$	Heat load,	W
Sp	The space between cylinder centers	m
CFD	Computational fluid dynamics	----

m/s.

CONCLUSION

The properties of fluid flow and forced convection heat transfer around a bank of eight circular cylinders in staggered arrangement implanted in a different porosity in two horizontal baked beds are investigated numerically in this analysis. In the porous channel and two porous baked beds, Reynolds numbers in the range of 1100 to 2250 and heat flux of 2000 W/m2 for various porous media types (Alumina, Silica Gel, and Molecular sieve 13x) are obtained .

The following results can be obtained from the current analysis:

As velocity rises, the air temperature rises faster along the flow direction, and the isotherm lines of the air travel closer to the cylinders' surfaces, resulting in higher temperature gradients.

When comparing the air velocity (0.187 m/s) example to the air velocity (0.35 m/s), the fluid thermal boundary layer around the cylinders is discovered to be quite thick. In current study, the interaction between porous particles and airflow causes the airflow pressure to drop dramatically as the diameter of porous particles increases.

As Alumina has a higher coefficient of thermal conductivity, porosity and permeability than Silica Gel and of Molecular Sieve 13X, it is more effective at lowering the surface temperature of the cylinder.

The study found that increasing the velocity from 0.187 m/s to 0.35 m/s resulted in considerable heat transfer between the air and the heater.

Nomenclature

References

[1] D. A. Nield and A. Bejan.1999. “Convection in Porous Media, Springer”.

[2] Bejan, A., Dincer, I., Lorente, S., Miguel, A.F., Reis, A.F.2004. “Porous and Complex Flow Structures in Modern Technologies”. Springer, New York .

[3] W.S. Wong, D.A.S. Rees, I. Pop, 2004. “Forced convection past a heated cylinder in a porous medium using a thermal non-equilibrium model: finite peclet number effects”, International Journal of Thermal Sciences Vol .43 No.3.

[4] M. Layeghi & A. Nouri-Borujerdi," Darcy Model for the Study of the Fluid Flow and Heat Transfer around a Cylinder Embedded in Porous Media", International Journal for Computational Methods in Engineering Science and Mechanics, 7:323–329, 2006.

[5] Gazy F. Al-Sumaily, Justin Leontini, John Sheridan and Mark C. Thompson. 2010. “Time-dependent fluid flow and heat transfer around a circular heated cylinder embedded in a horizontal packed bed of spheres” , AIP Conference Proceedings 1254, 331 .

[6] H.Y. Li , K.C. Leong , L.W. Jin , J.C. Chai .2010 . “Analysis of fluid flow and heat transfer in a channel with staggered porous blocks’’, International Journal of Thermal Sciences Vol .49, pp. 950-962.

[7] Khaled Al-Salem a, Hakan F. Oztop a, b, Suhil Kiwan c. “ Effects of porosity and thickness of porous sheets on heat transfer enhancement in a cross flow over heated cylinder’’. International Communications in Heat and Mass Transfer 38 (2011) 1279–1282.

[8] Forooghi, P., Abkar, M. & Saffar-Avval, M. 2011. “Steady and Unsteady Heat Transfer in a Channel Partially Filled with Porous Media under Thermal Non-Equilibrium Condition’’.,Transp Porous Med Vol. 86, pp. 177–198.

[9]H. J. Xu, Z. G. Qu, W. Q. Tao.2011. “Analytical solution of forced convective heat transfer in tubes partially filled with metallic foam using the two-equation model’’, International Journal of Heat and Mass Transfer, vol. 54, Issue 17-18, pp. 3846-3855.

[10] M. E. Nimvari, M. Maerefat, M. H. El-Hossaini.2012. “Numerical simulation of turbulent flow and heat transfer in a channel partially filled with a porous media’’, International journal of thermal sciences, vol. 60, pp. 131-141.

[11] Gazy F. Al-Sumaily, John Sheridan, Mark C. Thompson. 2012. “Analysis of forced convection heat

transfer from a circular cylinder embedded in a porous medium'', International Journal of Thermal Sciences Vol.51, pp. 121-131.

[12] Gazy F. Al-Sumaily, Mark C. Thompson. 2013. "Forced convection from a circular cylinder in pulsating flow with and without the presence of porous media'', International Journal of Heat and Mass Transfer Vol.61, pp. 226–244.

[13] Gazy F. Al-Sumaily.2014. "Forced convection heat transfer from a bank of circular cylinders embedded in a porous medium'', Journal of Heat Transfer, APRIL, Vol. 136.

[14] Sandeep Koundinya, Vigneshkumar N, A S Krishnan.2016. "Computational and experimental study of fluid flow and heat flow characteristics in porous media'', IOP Conf. Series: Materials Science and Engineering Vol .149 .

[15] Habib-Ollah Sayhvand , Ehsan Khalili dehkordi, and Amir Basir PAarsa. 2017. "Numerical analysis of forced convection heat transfer from two tandem circular cylinders embedded in a porous mediu'', Thermal Sciences , Vol. 21, No. 5, pp. 2117-2128.

[16] Brijendra Singh Bhaskar and S.K.Choudhary. 2017. "Experimental Investigation of Heat Transfer through Porous Material Heat Exchanger'', International Journal of Engineering Research and Technology. ISSN 0974-3154 Vol. 10, No. 1 , pp. 51-60.

[17] Mahboobe Mahdavi1, Saeed Tiari1, Ali Heidari, Majid Saffar Avval.2018. "Experimental and Numerical Study of Heat Transfer Enhancement in a Pipe partially or totally filled With A porous Material'', 3rd Thermal and Fluids Engineering Conference (TFEC) March 4–7, Fort Lauderdale, FL, USA, TFEC-2018-22071.

[18] Krishan Sharma, P. Deepu, Subrata Kumar.2020. "Convective heat transfer in a tube filled with homogeneous and inhomogeneous porous medium'', International Communications in Heat and Mass Transfer Vol. 117.

[19] Durlofsky, L., & Brady, J. F. (1987). "Analysis of the Brinkman equation as a model for flow in porous media'', *Physics of Fluids*, *30*(11), 3329.

[20]Leung CW, Chen S, Wong TT, Probert SD.2000. "Forced convection and pressure drop in a horizontal triangular sectional duct with V-grooved (i.e., orthogonal to the mean flow) inner surface''; Appl Energy;Vol. 66 , pp. 199–211.

[21]Jiyuan Tu, Guan-Heng Yeoh and Chaoqun Liu.2018. "Computational Fluid Dynamics" A Practical Approach Third Edition Elsevier Ltd, ISBN: 978- 0-08-101127-